



## Thermal Modelling of a Solar Air Heater for All Over the Year of Yazd Province

Safari <sup>a,\*</sup>, H., Dehghan <sup>a</sup>, A.

<sup>a</sup>School of Mechanical Engineering, Yazd University, Yazd-Iran.

\*E-mail: [Hediyeh\\_s2060@yahoo.com](mailto:Hediyeh_s2060@yahoo.com)

### ARTICLE INFO

Received: 20 August 2016  
 Received in revised form:  
 29 October 2016  
 Accepted: 30 October 2016

### Keywords:

Solar air heater;  
 Thermal modelling;  
 Energy efficiency

### A B S T R A C T

Solar collector, the first part of each solar dryer system, is important for industrial and agricultural purposes. The final objective of any solar system is to maximize its output. The energy analysis is excellent complementary thermodynamic tools for this purpose. In the present study, a comprehensive thermodynamic model for energy analysis of a double pass solar air heater has been carried out. Energy balance equations have been investigated for all components of the solar air heater including insulation, lower channel air stream, absorber, upper channel air stream and glass cover. The main object of this research was to find energy efficiency of a double-pass solar air heater for all over the year of Yazd Province in Iran. Moreover, the effect of inlet length and inlet width of collector on outlet temperature of solar air heater was studied. The results of the simulation showed that the maximum monthly average energy efficiency of the solar air heater is 32.41% in January with  $145 \text{ W/m}^2$  solar radiations. It is attributed to the fact that the inlet length of solar air heater has a positive effect on the increment of outlet temperature of top and bottom channel and efficiency of system, also the inlet width of solar air heater has negative effect.

© 2016 Published by University of Tehran Press. All rights reserved.

### 1. Introduction

Solar energy is so useful and a good source for energy applications. This source depicts a new kind of energy without any pollution, inexhaustibility and its multitude, so it can be found normally in a lot of areas on the earth. It usually does not want shrill utensil, which is why we can exhaust it in many places. However, high cost and low availability of solar energy is more excessive in compared with other energy sources, but above reasons justify its usage.

Yazd is located in an appropriate station geographically as to solar radiation. Therefore, using solar energy is a suitable solution to extend the renewable energies and to stop environmental impacts due to the fossil fuels. Zarezade and Mostafaeipour [1] have studied the solar dryer feasibility which are used to dry fruits, vegetables and agriculture products for Yazd province. All factors and risks influencing these solar dryer have been identified.

Thermal energy can be exploited solar energy by using flat plate solar collectors which are used for moderate and low temperature applications [2]. K.S.ONG [3] performed mathematical model of thermal performance of four types of flat plate solar air collectors. The effects of wind and film heat transfer coefficients on the solar air heater were discussed. According to the experimental and theoretical investigations, the best configuration for solar air heater is double-pass solar collector with a quarter perforated cover [4, 5]. Various theoretical and

experimental investigations have been performed to increase thermal performance of the double pass solar air heaters. A comprehensive review was conducted on thermal performance of double pass solar air heaters [2, 5], shows the double pass solar air heaters perform better than the single pass solar air heater owing to the reduced thermal losses [4-7]. The single pass and double pass solar air heater with four transverse fins was tested by A.J. Mahmood et al [7], according to its results, with decreasing the air mass flow rate, the temperature difference between the inlet and outlet increases.

Many studies have been done to make solar air heaters more reliable, efficient, and cost effective for all applications. Roozbeh Vaziri [8] experimentally investigated thermal performances of different inner collector colors. Sunil Chamolia et al [9] presented a brief review of the performance double passes solar air heater and the different methods those amplify their operation and theoretical models of double pass solar air heaters. The packing material, mass flow rate of air, recycle ratio, fins integrated double pass solar air heater are considered the important parameters of double pass solar air heater. Saxena et al [10] reported various methods which are used to improve performance of solar air heaters such as: use of protracted surfaces with varied dimensions and shapes, optimizing the dimensions of the construction elements, integrating heaters with the photovoltaic elements, etc. Chii-Dong Ho et al [11] performed theoretical and experimental investigation of wire mesh

packed double-pass solar air heaters with external recycle. The wire mesh packed solar air heater leads turbulence intensity and broaden the heat transfer area, so the heat transfer efficiency in enhanced. A comprehensive revisal of reported studies imply that the thermal performance of double pass solar air heaters with packed bed material in the upper channel increases as compared to solar air heater with packed bed material in lower channel and without packed bed [6]. Anil SinghYadav et al [12] discussed a detailed review of the experimental investigations in order to improve the heat transfer by the use of artificial roughness of various sizes, shapes and orientations in design of solar air heater. The use of artificial roughness to increase heat transfer on a surface in the duct is an effective technique.

Before installing real experimental configuration, the new numerical methods permits researchers to perform the critical flow analysis and allows researchers to simulate two and three dimensional computational of solar air heater. A detailed discussion about the usage of CFD in the analysis of solar air heater duct carried out in the literature was presented in 2016 (Vipin B.Gawande et al) [13].

In this research, we attempted a theoretical study of double pass solar air heater for allover the year using experimental data of Yazd province in Iran. The first, mathematical modeling of energy balanced have been performed and then analysis the effect of some parameters on the temperature and efficiency of this model.

## 2. Materials and Methods

Solar collector is the main components of all solar systems. The schematic of heat transfer in the solar air heater is shown in Fig. 1. In this modeling solar air heater was divided into two channels. The first channel extended from glass cover to absorber. The second channel extended from absorber to insulation.

The various assumptions made for energy balance are as follows:

1. Air with environment temperature will enter to up and bottom channel.
2. The solar air heater operation is under steady-state condition.
3. Solar radiation is assumed as monthly averages, which the data used is for Yazd province.

### 2.1. Thermal network

The thermal network for this type of solar collector indicates in Fig. 2. Using the above assumptions energy balance equations may be expressed as:

1. Heat balance on glass

$$h_{ru}A(T_o - T_g) + \alpha_1 SA + h_g A(T_{au} - T_g) = h_w A(T_g - T_\infty) + h_{rs} A(T_o - T_s) \quad (1)$$

2. Heat balance on the absorber

$$S \tau \alpha_1 A = h_u A(T_o - T_{au}) + h_{ru} A(T_o - T_g) + h_{ul} A(T_o - T_{al}) + h_{rb} A(T_o - T_b) \quad (2)$$

3. Heat balance on the upper part of insulation

$$h_{rb} A(T_o - T_b) + h_b A(T_{al} - T_b) = (T_b - T_\infty) / [1 / ((L_1 / t_{c1}) + (1 / h_w))] \quad (3)$$

4. Heat balance on upper channel air stream

$$m_1 c_p (T_{au} - T_{ai}) = h_u A(T_o - T_{au}) - h_g A(T_{au} - T_g) \quad (4)$$

5. Heat balance on lower channel air stream

$$m_2 c_p (T_{ale} - T_{ali}) = h_u A(T_o - T_{al}) - h_b A(T_{al} - T_b) \quad (5)$$

6. Average temperature of upper air stream can be expressed as:

$$T_{au} = (T_{aue} + T_{aui}) / 2 \quad (6)$$

7. Average temperature of lower air stream can be expressed as:

$$T_{al} = (T_{ale} + T_{ali}) / 2 \quad (7)$$

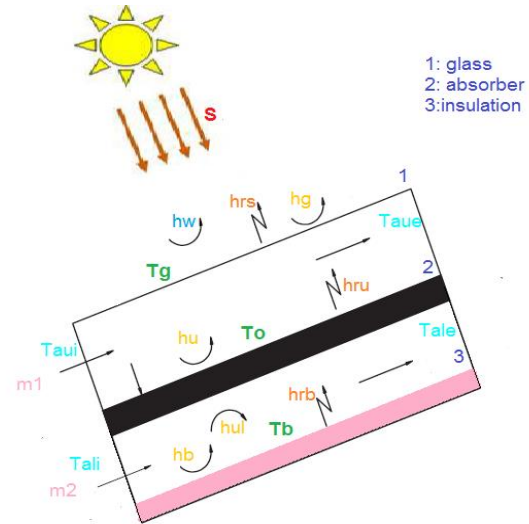


Figure 1. Schematic of solar air heater with heat transfer coefficients.

### 2.2. Radiation heat transfer coefficient from top and bottom surfaces

The radiation heat transfer coefficient from upper cover to sky referred to the ambient temperature can be fine as

$$h_{rs} = \sigma \alpha_1 (T_g^4 - T_s^4) / (T_g - T_\infty) \quad (8)$$

To obtain the sky temperature is given by [14]  $T_s = 0.0552 T_\infty^{1.5}$

$$(9)$$

### 2.3. Heat transfer coefficient for wind

The convection heat transfer coefficient due to wind obtained using McAdams correlation [9]

$$h_w = 5.7 + 3.8V \quad 0 < V < 3 \quad (10)$$

### 2.4. Radiation heat transfer between parallel plates

The radiation heat transfer coefficients between two Plates set glass-absorber and absorber insulation are given as

$$h_{ru} = \frac{\sigma (T_g^2 + T_o^2) (T_g + T_o)}{(1 / \epsilon_1 + 1 / \epsilon_2 - 1)} \quad (11)$$

and

$$h_{rb} = \frac{\sigma (T_b^2 + T_o^2) (T_b + T_o)}{(1 / \epsilon_3 + 1 / \epsilon_4 - 1)} \quad (12)$$

### 2.5. Convection heat transfer coefficient for plates

The convective heat transfer coefficient for glass is calculated by using the non-dimensional Nusselt number as [14]

$$h_g = \frac{N_u K_g}{L} \quad (13)$$

Similar to the present model for convective heat transfer coefficient, various models have been also calculated like this to

estimate the convection heat transfer coefficient as  $h_u$ ,  $h_{ul}$  and  $h_b$ .

### 2.6. Forced convection heat transfer coefficient

By knowing flow region as turbulent for the local Nusselt number, it can be found template equations of entrance air stream for heat transfer coefficient calculations.

#### 2.6.1. Turbulent flow region ( $Re > 6000$ )

The heat transfer in the developed flow region should be obtained as [9]

$$N_{u_\infty} = 0.018 Re_f^{0.8} Pr^{0.4} \quad (14)$$

for  $9500 < Re < 22,000$

$$N_u = 0.027 Re_f^{0.8} Pr^{1/3} (\mu_f / \mu_w)^{0.14} \quad (15)$$

#### 2.6.2. Entrance region ( $Re > 10,000, L / D_h < 60$ )

By studying on effect of the thermal entrance region on turbulent, Nusselt Number can be determine as [15]

$$N_u = N_{u_\infty} (1 + S D_h / L) \quad (16)$$

where the factor  $S$  represented by [9]

$$S = 14.31 \text{Log}(L / D_h) - 7.9 \quad (17)$$

hydraulic diameter defined as [9]

$$D_h = \frac{4A_c}{P} \quad (18)$$

$$Q_{al} = m \dot{c}_p (T_{ale} - T_{ali}) / A_c \quad (24)$$

for both air streams, the heat collection energy is obtained by adding the individual air stream efficiencies

$$Q_{tot} = Q_{au} + Q_{al} \quad (25)$$

To find the efficiency of the system, the ratio of total energy absorbed by air in both channels to the solar radiation should be calculated

$$\eta = \frac{Q_{tot}}{\text{solar radiation}} \quad (26)$$

Table 2 reports the monthly average of temperature and solar radiations for Yazd province in Iran that is used in the efficiency calculation. The above equations were solved using EES program software.

## 3. Results & Discussion

Table 1 illustrates the effect of solar radiation and temperature of different months of the year on average temperature of top and bottom air channel and efficiency of the system. The Maximum temperature difference between top and bottom channel is around 1.1K, which happened in January, with maximum solar radiation ( $331 \text{ W/m}^2$ ). Hence, the total heat energy of the system is highest in January. Also, the heat energy of top channel is higher than the bottom channel throughout the year. According to the results presented in Table 1, the efficiency of solar air heater is not so different all over the year. The maximum values of energy efficiency were found 32.41% and 32.11% respectively. As it is obvious, the most efficiency is obtained in January and December with lowest solar radiation. It is also seen that the minimum efficiency of this solar air heater is in August and then September.

Fig. 2 shows the effect of inlet length variation of collector on average temperatures and exit temperatures of top and bottom channels. It is seen in the range of 0.85-1.35m, the temperature of top channel increases from 345K to 347.3K (about 0.67%) and the temperature of bottom channel increases about 0.64% in this interval.

The hydraulic diameter  $D_c$  for parallel flat plates is distance between the plates

### 2.7. Physical properties

Because of the low temperature, the physical properties of air are assumed to vary linearly with temperature  $T_m$  (K), so the relationships obtained as [9]

viscosity

$$\mu = [1.983 + 0.00184(T_m - 300)]10^{-5} \quad (19)$$

density

$$\rho = 1.1774 + 0.00359(T_m - 300) \quad (20)$$

thermal conductivity

$$\kappa = 0.02624 + 0.0000758(T_m - 300) \quad (21)$$

specific heat

$$c = 1.0057 + 0.000066(T_m - 300) \quad (22)$$

### 2.8. Efficiency

For a collector of length L, the heat energy of the first air stream is defined as

$$Q_{au} = m \dot{c}_p (T_{aue} - T_{aui}) / A_c \quad (23)$$

and for the second air stream, is given by

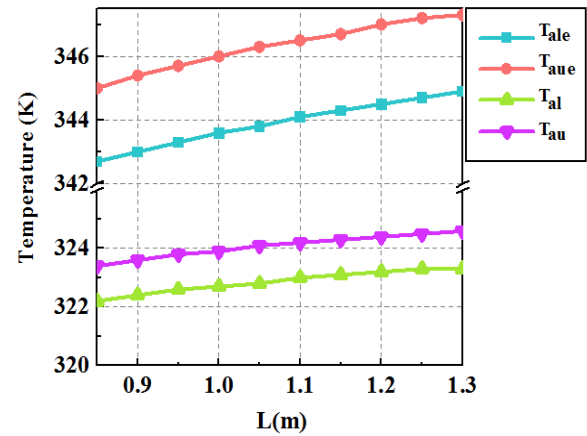


Figure 2. Effect of inlet length variation of collector on value of top and bottom channel temperatures.

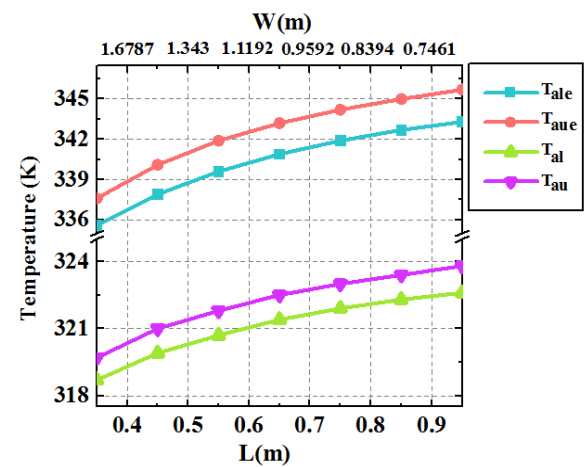


Figure 3. Effect of length variation and inlet width variation of collector on value of top and bottom channel temperatures with fixed area ( $A = 0.6715 \text{ m}^2$ ).

Table 1. Solar air heater temperatures and its efficiencies in different months of the year.

MOUNTH	T(K)	solar radiation ( W/m <sup>2</sup> )	T <sub>au</sub> (K)	T <sub>al</sub> (K)	Q <sub>au</sub>	Q <sub>al</sub>	Q <sub>tot</sub>	η
Jan.	279.13	145	289.7	289.5	46.991	23.33	23.662	32.41
Feb.	282.56	195.6	296.6	296.2	62.802	30.953	31.849	32.11
Mar.	287.28	208	301.6	301.2	65.095	32.093	33.003	31.3
Apr.	293.49	228	308.7	308.2	70.093	34.467	35.627	30.74
May.	298.71	302.5	318.4	317.5	91.494	44.568	46.926	30.25
Jun.	303.84	331	324.8	323.7	98.762	48.003	50.759	29.84
Jul.	305.99	322	325.9	325	94.712	46.21	48.502	29.41
Aug.	304.03	310.2	322.7	322	88.533	43.367	45.165	28.54
Sep.	300	264.7	316.4	316	77.441	38.247	39.194	29.26
Oct.	293.84	203	306.9	306.7	60.881	30.266	30.614	29.99
Nov.	286.83	151.8	297	297	46.718	23.359	23.359	30.78
Dec.	281.67	119	289.9	289.9	37.473	18.792	18.68	31.49

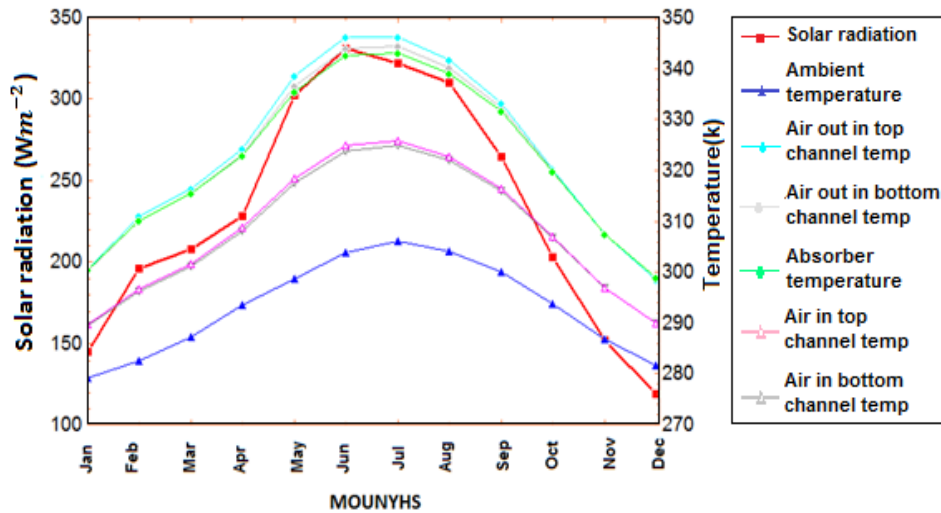


Figure 4. Monthly variation of solar radiation and temperature of solar air heater components.

As it is obvious,  $T_{al}$  and  $T_{au}$  have a perspicuous increment from 0.85 m to 1.35 m. The temperature increase has a direct impact on increasing efficiency and the efficiency of solar heater is enhanced.

The effect of L and W are investigated for top and bottom channel temperatures depicted in Fig. 3, while the inlet area is assumed to be constant. According to this Fig, the increment of W (inlet width) from 0.7461m to 1.6787m causes the decrease of all temperatures. So, W has negative effect on  $T_{al}$ ,  $T_{au}$ ,  $T_{ale}$  and  $T_{aue}$ . The increment of L (from 0.35m to 0.95m) and decrement of W (from 1.6787m to 0.7661m) cause the increment of  $T_{ale}$  and  $T_{aue}$  within 2.29% and 2.39%.

It can be seen that the most solar radiation exists in June for Yazd province. Fig.4 shows the monthly solar intensity and the temperature values of ambient; Air out in top and bottom channels, absorber and average temperature of top and bottom channel. It is seen that at the time of maximum solar radiation, maximum air temperatures will occur in top and bottom of channel output in June. Also, The higher temperature difference between up and low channel is about  $2.3^{\circ}\text{C}$ . Results also show that the temperature output and average temperatures of upper channel is higher than low channel in all over the year because of higher heat capacity of the absorption of solar radiation in the glass. The average air temperature curve in top and low channels and the ambient temperature curve have approximately the same trend, but ambient temperature is lower than average channel temperatures as expected.

#### 4. Conclusions

In present study, theoretical modeling of heat transfer in the solar collector was investigated. The energy balance equations of solar air heater were written with compute

heat transfer coefficients. The ambient conditions and solar radiation of Yazd province in Iran were used to

perform modeling on solar air heater. The monthly average energy efficiency has been calculated. It was found that, the monthly energy efficiency is partly lower in August than other months and the highest monthly average efficiency detected in January with  $145 \text{ W/m}^2$  solar radiations. Furthermore Result showed the increment of inlet length and inlet width of solar collector has a positive and negative effect respectively on outlet temperature of solar air heater.

#### Nomenclature

A	area of each plate( $\text{kgm}^{-3}$ )
h	heat transfer coefficient ( $\text{Wm}^{-2}\text{C}^{-1}$ )
h <sub>b</sub>	heat transfer coefficient for bottom part of insulation ( $\text{Wm}^{-2}\text{C}^{-1}$ )
	area of each plate ( $\text{kgm}^{-3}$ )

$h_g$	heat transfer coefficient for glass ( $\text{Wm}^{-2}\text{C}^{-1}$ )
$h_{rb}$	radiation heat transfer coefficient in bottom channel( $\text{Wm}^{-2}\text{C}^{-1}$ )
$h_{ru}$	radiation heat transfer coefficient in upper channel( $\text{Wm}^{-2}\text{C}^{-1}$ )
$h_u$	heat transfer coefficient for upper part of absorber ( $\text{Wm}^{-2}\text{C}^{-1}$ )
$h_{ul}$	heat transfer coefficient for lower part of absorber ( $\text{Wm}^{-2}\text{C}^{-1}$ )
$h_w$	heat transfer coefficient for wind ( $\text{Wm}^{-2}\text{C}^{-1}$ )
$L_1$	thickness of insulation(m)
$m_1$	mass flow in upper channel( $\text{kgs}^{-1}$ )
$m_2$	mass flow in lower channel( $\text{kgs}^{-1}$ )
$Q_{au}$	heat energy of upper air stream channel( $\text{Wm}^{-2}$ )
$Q_{al}$	heat energy of lower air stream channel( $\text{Wm}^{-2}$ )
$Q_{tot}$	total heat energy of air channels( $\text{Wm}^{-2}$ )
$S$	solar radiation falling on solar air heater under consideration( $\text{Wm}^{-2}$ )
$T_{al}$	average temperature of air in lower channel(K)
$T_{ale}$	exit temperature of air in lower channel(K)
$T_{ali}$	initial temperature of air in lower channel
$T_{au}$	average temperature of air in upper channel(K)
$T_{aue}$	exit temperature of air in upper channel(K)
$T_{aui}$	initial temperature of air in upper channel(K)
$T_b$	temperature of bottom insulation(K)
$t_{c1}$	thermal conductivity of insulation ( $\text{Wm}^{-1}\text{C}^{-1}$ )
$T_g$	temperature of glass(K)
$T_\infty$	ambient temperature(K)
$T_o$	temperature of absorber(K)
$T_s$	temperature of sky(K)

$V$	wind velocity( $\text{ms}^{-1}$ )
$\alpha_1$	absorption for glass
$\alpha_2$	absorption for absorber
$\eta_{tot}$	efficiency
$\sigma$	Stefan-Boltzmann constant ( $5.67*10^{-8}\text{Wm}^{-2}\text{K}^{-4}$ )
$\tau$	transmittance
$\rho$	density of air( $\text{kgm}^{-3}$ )
$\mu$	dynamic viscosity of air ( $\text{kgm}^{-1}\text{s}^{-1}$ )
$\kappa$	thermal conductivity of air( $\text{Wm}^{-1}\text{K}^{-1}$ )
$\varepsilon_1$	emissivity of top glass surface
$\varepsilon_2$	emissivity of absorber upper surface
$\varepsilon_3$	emissivity of absorber lower surface
$\varepsilon_4$	emissivity of bottom plate surface

## References

1. Ozturk, M. and I. Dincer, *Thermodynamic analysis of a solar-based multi-generation system with hydrogen production*. Applied Thermal Engineering, 2013. **51**(1): p. 1235-1244.
2. Ravi, R.K. and R.P. Saini, *A review on different techniques used for performance enhancement of double pass solar air heaters*. Renewable and Sustainable Energy Reviews, 2016. **56**: p. 941-952.
3. Ong, K., *Thermal performance of solar air heaters: mathematical model and solution procedure*. Solar energy, 1995. **55**(2): p. 93-109.
4. Nowzari, R., N. Mirzaei, and L. Aldabbagh, *Finding the best configuration for a solar air heater by design and analysis of experiment*. Energy Conversion and Management, 2015. **100**: p. 131-137.
5. Nowzari, R., L. Aldabbagh, and F. Egelioglu, *Single and double pass solar air heaters with partially perforated cover and packed mesh*. Energy, 2014. **73**: p. 694-702.
6. Singh, S. and P. Dhiman, *Thermal performance of double pass packed bed solar air heaters—A comprehensive review*. Renewable and Sustainable Energy Reviews, 2016. **53**: p. 1010-1031.
7. Mahmood, A., L. Aldabbagh, and F. Egelioglu, *Investigation of single and double pass solar air heater with transverse fins and a package wire mesh layer*. Energy Conversion and Management, 2015. **89**: p. 599-607.
8. Vaziri, R., M. İlkan, and F. Egelioglu, *Experimental performance of perforated glazed solar air heaters and unglazed transpired solar air heater*. Solar Energy, 2015. **119**: p. 251-260.
9. Chamoli, S., et al., *A review of the performance of double pass solar air heater*. Renewable and

- Sustainable Energy Reviews, 2012. **16**(1): p. 481-492.
10. Saxena, A. and A. El-Sebaei, *A thermodynamic review of solar air heaters*. Renewable and Sustainable Energy Reviews, 2015. **43**: p. 863-890.
  11. Ho, C.-D., et al., *Performance improvement of wire mesh packed double-pass solar air heaters with external recycle*. Renewable energy, 2013. **57**: p. 479-489.
  12. Yadav, A.S. and M.K. Thapak, *Artificially roughened solar air heater: Experimental investigations*. Renewable and Sustainable Energy Reviews, 2014. **36**: p. 370-411.
  13. Gawande, V.B., et al., *A review of CFD methodology used in literature for predicting thermo-hydraulic performance of a roughened solar air heater*. Renewable and Sustainable Energy Reviews, 2016. **54**: p. 550-605.
  14. Chan, Y., N. Dyah, and K. Abdullah, *Performance of a Recirculation Type Integrated Collector Drying Chamber (ICDC) Solar Dryer*. Energy Procedia, 2015. **68**: p. 53-59.